Int. J. Electrochem. Sci., 14 **(2019)** 5521 – 5534, doi: 10.20964/2019.06.13

International Journal of ELECTROCHEMICAL SCIENCE
www.electrochemsci.org

Investigation on Degradation and Viscoelastic Relaxation of Li Ion in Chitosan Based Solid Electrolyte

Shujahadeen B. Aziz[1,2*], *M. A. Brza*[3,1], *M. F. Z. Kadir*[4], *M. H. Hamsan*[4], *Z. H. Z. Abidin4*, *Dana A. Tahir*[5], *Omed Gh. Abdullah*[1,2]

[1] Advanced Polymeric Materials Research Lab., Department of Physics, College of Science, University of Sulaimani, Qlyasan Street, Sulaimani, Kurdistan Regional Government-Iraq
[2] Development Center for Research and Training (DCRT), University of Human Development, Qrga Street, Sulaimani, Kurdistan Regional Government-Iraq
[3] Faculty of Engineering, International Islamic University of Malaysia, kuala Lumpur, Gombak, Malaysia
[4] Centre for Foundation Studies in Science, University of Malaya, Kuala Lumpur, Malaysia
[5] College of Science, Physics Department, University of Halabja, Halabja, Kurdistan Regional Government-Iraq
[*]E-mail: shujaadeen78@yahoo.com, shujahadeenaziz@gmail.com

Received: 22 Janaury 2019/ *Accepted:* 16 March 2019 / *Published:* 10 May 2019

Ion transport has been the subject of debate among scientists for more than three decades. This paper discusses the preparation, degradation and viscoelastic relaxation dynamics of ions in chitosan-based solid electrolyte. The dielectric properties and viscoelastic relaxation process of chitosan:$LiCF_3SO_3$ (CS:LiTf) solid electrolyte were examined by means of electrochemical impedance spectroscopy (EIS). The high values of dielectric constant (ε′) and dielectric loss (ε″) at low frequency were ascribed to electrode polarization phenomena. The decrease of both ε′ and ε″ at higher temperatures could be ascribed to the degradability of chitosan-based solid electrolyte. The real part of electrical modulus shows that CS:LiTf system is highly capacitive. The asymmetric peak of the imaginary part (*M″*) of electric modulus suggests the non-Debye type of relaxation. The frequency dependence of dielectric loss (ε″) and imaginary part (*M″*) of electric modulus revealed good coupling between polymer segmental and ionic motions. The master curve obtained from the scaling of M" spectra at various temperature was helpful in understanding the dielectric processes taking place in the CS:LiTf electrolyte. The temperature dependence of the conductivity relaxation time (τ_σ) follows the Arrhenius equation. The viscoelastic relaxation dynamic of the chitosan-based solid electrolyte was investigated by two methods.

Keywords: Polymer electrolyte; Degradation; Dielectric constant; Dielectric loss; Electric modulus; Scaling; viscoelastic relaxation; Ion dynamics.

1. INTRODUCTION

A major topic within research concerned with secondary lithium batteries is the evolution of harmless electrolytes, and especially solid polymer electrolytes (SPEs), even though knowledge about this class of compounds has existed for nearly four decades [1]. Ion-conducting polymers derived from dissolved salts in functional polymers have received growing attention due to their application in electrochemical devices [2]. Solid polymer electrolytes based on natural polymers are harmless to the environment and have attracted substantial interest recently owing to their possible uses in electrochemical devices (e.g. electrochromic devices, high-energy density batteries, sensors and fuel cells) [3, 4]. Extensive research has also been dedicated to biodegradable natural polymers (e.g. starch, cellulose, chitosan, carrageenan, agarose) in recent times because of their environmental sustainability and ease of use in the preparation of electrolytes [5]. After cellulose, the second most abundant biopolymer in nature is chitin and its deacetylated product is chitosan (CS) [6]. Chitosan derived from shrimp waste as a natural polymer and has received substantial interest in many potential applications [7] as well as it is a polycationic polymer with an amino group and two hydroxyl groups in the repeating unit [8, 9]. The properties of biocompatibility, biodegradability, minimal toxicity and inexpensiveness make chitosan an attractive biomaterial [10]. Furthermore, chitosan generally possesses high molecular weight polysaccharide and strong network of intermolecular or intramolecular hydrogen bonds [11] and, despite presenting a crystalline structure and several hydrogen bonds, it is usually soluble in acids [12].In the field of condensed matter physics, a subject that has been the focus of extensive investigation based on dielectric relaxation analysis in polymer electrolytes is ion dynamics [13-16]. The investigation of dielectric relaxation in solid polymer electrolytes is a powerful approach for achieving knowledge about the characteristics of ionic and molecular interactions [17]. The co-existence of crystalline and amorphous phases in polymer electrolytes (PEs) is well known, with the amorphous phase being the site where ion conduction primarily occurs [18, 19]. The AC electrical investigation of polymers reveal some structural details and supply important complementary information to the use of polymer materials for electrical purposes [20].

Under environmental conditions, polymeric materials suffer the loss of their natural properties as they degrade due to the effect of light, heat and so on [21]. The structure, relaxation dynamics and degradability of polymeric systems can be effectively investigated through the highly sensitive electrical impedance spectroscopy [22, 23]. To the best of our knowledge, the degradation and origin of the relaxation process in chitosan-$LiCF_3SO_3$ (CS:LiTf) solid electrolyte have not been researched so far, which is why this study focuses on degradation and ion relaxation dynamics by undertaking analysis of temperature-dependent dielectric properties and electric modulus. To improve knowledge of ion dynamics in CS-based polymer electrolyte, the electric modulus was normalized.

2. EXPERIMENTAL METHOD

2.1 Materials and sample preparation

The raw materials employed for the purposes of the present research were chitosan from crab shells (≥75% deacetylated, Sigma Aldrich) and lithium triflate with a molecular weight of 256.94 (≥98

purity, Fluka). The solution cast technique was used with acetic acid (1%) as solvent to prepare the solid polymer electrolyte (SPE) films. Within this system, 1g chitosan was fixed and dissolved in acetic acid solution, followed by addition of 8wt% lithium triflate (LiTf) to prepare the CS:LiTf-based solid electrolyte. Homogeneous solutions were achieved through continuous stirring of the mixtures. The solution was cast in a Petri dish and allowed to dry at ambient temperature to enable formation of films. For further drying, the formed films were transferred in a desiccator.

2.3 Impedance measurement

The HIOKI 3531 Z Hi-tester interfaced to a computer was employed for the measurement of film impedance under conditions of 50Hz-100kHz frequency range and 303-413K temperature range. The measurement was controlled by the software, which also determined the real and imaginary parts of impedance. The SPE films were cut into small discs with diameter of 2cm and sandwiched between two stainless steel electrodes under spring pressure. The real and imaginary parts of complex permittivity (ε*) and complex electric modulus (M*) were determined based on the real (Z') and imaginary (Z") parts of the complex impedance (Z*).

3. RESULTS AND DISCUSSION

3.2 Dielectric analysis

3.2.1 Frequency and temperature dependence of ε′ and ε″

The conductivity and dielectric behavior of polymer electrolytes can be effectively investigated through dielectric spectroscopy. The formulae below were employed to determine the real and imaginary parts of complex permittivity (ε*) based on the real (Z') and imaginary (Z") part of complex impedance (Z*) [24, 25]:

$$\varepsilon' = \frac{Z''}{\omega C_\circ (Z'^2 + Z''^2)} \quad (1)$$

$$\varepsilon'' = \frac{Z'}{\omega C_\circ (Z'^2 + Z''^2)} \quad (2)$$

In the above equations, the dielectric constant is denoted by ε′, while the dielectric loss is denoted by ε″. The vacuum capacitance C_o is derived from $\varepsilon_o A/t$, with thickness and area of the film being respectively denoted by t and A. ω represents the angular frequency corresponding to 2πf, with f denoting the applied field frequency.

The dielectric constant and dielectric loss are illustrated in Figures 1 and 2 as a function of frequency at various temperatures, being apparent that a rise in temperature determines an increase in dielectric constant as well as dielectric loss. Another observation that can be derived is that, at low

frequency, dielectric constant and dielectric loss are high as a result of electrode polarisation phenomena [26-28]. The electrode polarization is the local accumulation of identical charges from drifting across the materials. Electrode polarisation takes place at the interface between two materials with different dielectricity or conductivity. Meanwhile, the charge carriers have less time to drift with the increase in frequency, leading to reduction in dielectric constant and dielectric loss [29-32]. The outcome is a decline in and eventual vanishing of the polarizability contribution from ionic and orientation sources owing to the inertia of the ions [33]. As can be seen, due to the contribution of DC conductivity to the values of dielectric loss [34, 35], dispersion in dielectric constant spectra begins from log(f)=3, whereas dispersion in dielectric loss spectra is stronger and begins from log(f) that is almost 4.

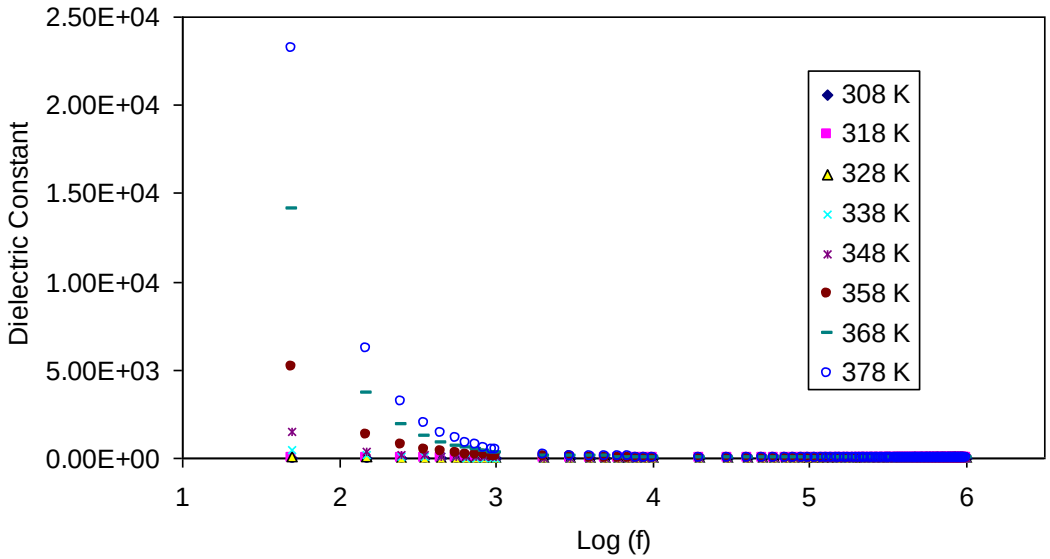

Figure 1. Frequency dependence of dielectric constant (ε′) at selected temperatures for CS:LiTf system. Clearly the dielectric constant increases with temperature rise.

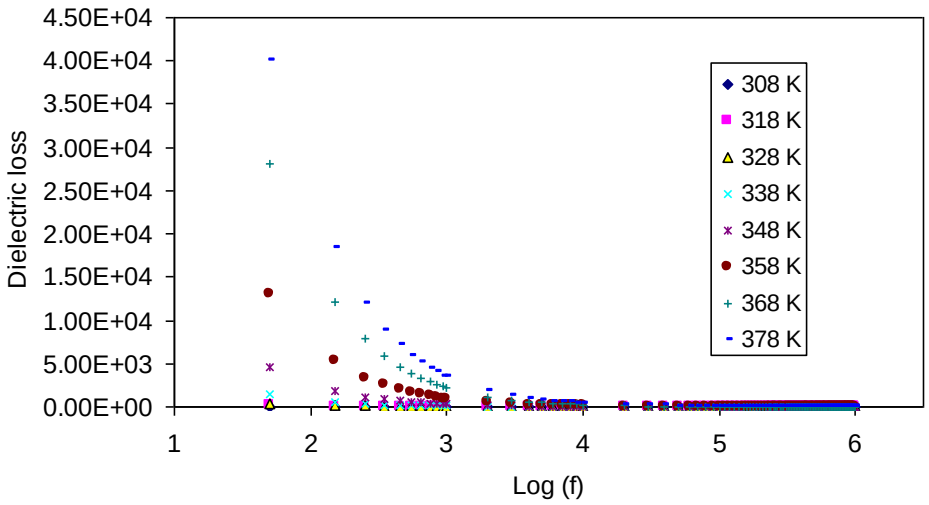

Figure 2. Frequency dependence of dielectric loss (ε″) at selected temperatures for CS:LiTf system. The dispersion in dielectric loss spectra increases with increasing temperature.

Figure 3 and Figure 4 respectively illustrate the temperature dependence of the dielectric constant and dielectric loss at varying frequencies, clearly showing that rise in temperature up to 393K causes an increase in both dielectric constant and dielectric loss, whilst after this value, the rise in temperature causes a decrease in dielectric constant and dielectric loss. The increase of solid electrolyte dielectric constant and dielectric loss with increase in temperature is usually related with the reduction in bond energies and intensification of polarisation [32, 33]. This is associated with the fact that the presence of forces in polymer materials are classified into primary (intra-chain) and secondary (inter-chain) forces that are intended to stabilize the polymer structure [36]. The chain backbone atoms are linked by covalent bonding (2.2-8.6eV), which is the source of the primary forces. As regards secondary forces, four distinct ones occur in polymers, namely, ionic bonding (0.43-0.87 eV), hydrogen bonding (0.13-0.30 eV), dipolar interaction (0.07-0.13 eV) and Van der Waals interaction (0.002-0.09 eV). Compared to their primary counterpart, secondary forces display greater temperature dependence because of their low dissociation energies and have a major impact on the nature and extent of molecular movements within polymers, which influence their dielectric behavior, charge transport and charge storage properties. Therefore, there is an increase in the degree of salt dissociation and re-dissociation of ion aggregates with rise in temperature, from which it can be deduced that the free ion number or charge carrier density increases [37]. As a result, up to the temperature value of 393K, there is an increase in both dielectric constant and dielectric loss. At low frequencies, ε' and ε" have a high value that suppresses the values of ε' and ε" at high frequencies, obscuring the appearance of their peaks. This may provide an explanation for the constant value of dielectric constant and dielectric loss at higher frequencies as a temperature function. It is also important to note that, by comparison to dielectric constant, dielectric loss increases faster as the temperature rises, which can be ascribed to the two contributions that dielectric loss has from the dielectric polarization processes and from the DC conduction, respectively [38]. As shown in Figure 4, the loss factor participated by dc conductivity increases with the rise in temperature and dominates at high temperature.

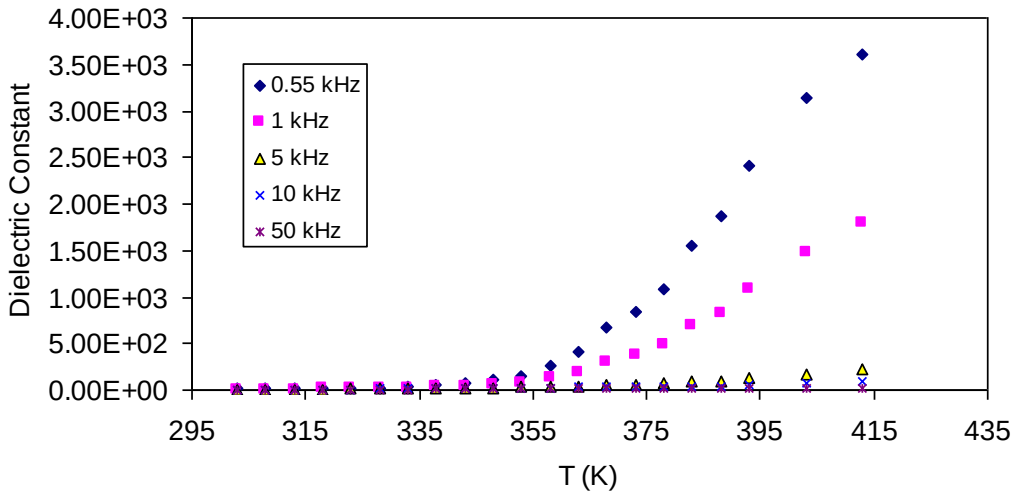

Figure 3. Temperature dependent of dielectric constant (ε′) at selected frequencies. Degradation in dielectric constant have been appeared at high temperature.

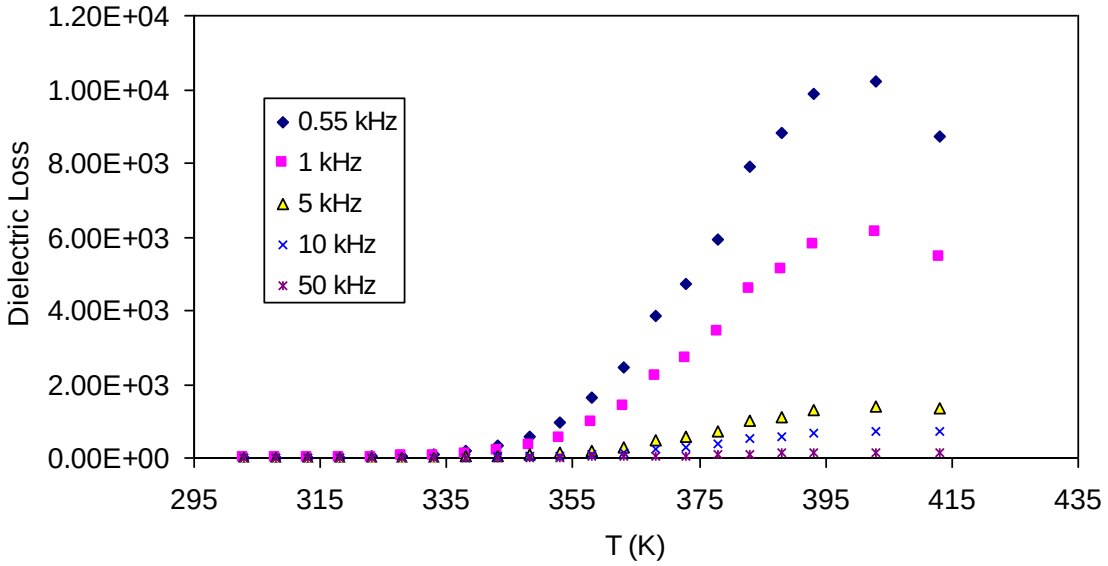

Figure 4. Temperature dependent of dielectric loss (ε″) at selected frequencies. Degradation in dielectric loss have been appeared at high temperature due to water desorption.

As temperature rises beyond 393K, there is a reduction in both ε′ and ε″, which is likely due to the presence of water molecules bound by polar groups (hydroxyl and amine groups) in chitosan [39]; more specifically, elimination of water molecules at lower temperature is difficult because chitosan membranes are hydrophilic materials. Although adhesion could be beneficial at lower temperature, water desorption occurs as temperature rises, disrupting the natural properties of chitosan-based solid membranes, which thus become hard membranes. Under such circumstances, there is an increase in the interfacial resistance between electrodes and membranes, which in turn enhances membrane resistance at higher temperature [40]. Consequently, the adhesiveness between membrane and electrode is diminished due to water desorption at high temperature [41], leading to a reduction in ε′ as well as ε″. Another observation is that, during of heat treatment, the colour of the membrane changed to a dark brownish and become hard and shrunk due to water desorption, as well as nearly brittle by comparison to the original membrane before EIS treatment. As such, it is significant from both a scientific and industrial perspective to have comprehension of the thermal degradation of polymeric materials for device application. To the best of our knowledge, this is the first report that predicts the degradation of chitosan based solid electrolyte from dielectric analysis.

3.3 Electric modulus analysis

3.3.1 Frequency dependence of M' and M" at selected temperatures

Insight into bulk relaxation properties at low frequencies can be achieved based on the electric modulus, which can make it possible to address or disregard common obstacles such as electrode

nature, space charge phenomena and conduction effects that seem to obscure relaxation in permittivity presentation [15, 41-44]. According to recent research evidence, both the frequency-dependent conductivity and relaxation dynamics are sensitive to the movement of charge species and dipoles of the polymer electrolytes [42-44]. Investigation of dielectric relaxation in electric modulus formalism can help to examine relaxation dynamics in detail [44]. The relations below were applied to determine the real and imaginary parts of complex electric modulus (M^*) based on the real (Z') and imaginary (Z'') part of complex impedance (Z^*) [43, 44].

$$M' = \frac{\varepsilon'}{(\varepsilon'^2 + \varepsilon''^2)} = \omega C_o Z'' \quad (3)$$

$$M'' = \frac{\varepsilon''}{(\varepsilon'^2 + \varepsilon''^2)} = \omega C_o Z' \quad (4)$$

The frequency dependence of the electric modulus real part M' at various temperatures for the sample displaying the highest dielectric constant is illustrated in Figure 5. The figure clearly shows the long tail of the M' spectra at low frequency which can be ascribed to the large capacitance related to the solid electrolyte [45, 46]. Low $M_r$values at low down frequencies at selective temperatures, indicate the lack of appreciable electrode polarization [47].In contrast to permittivity, the M′ decreases as the temperature rises, which is due to the fact that, as the temperature increases, the mobility of the polymer segment and charge carriers increases as well. Hence, increase in conductivity leads to a reduction in Z′ as well as Z″.

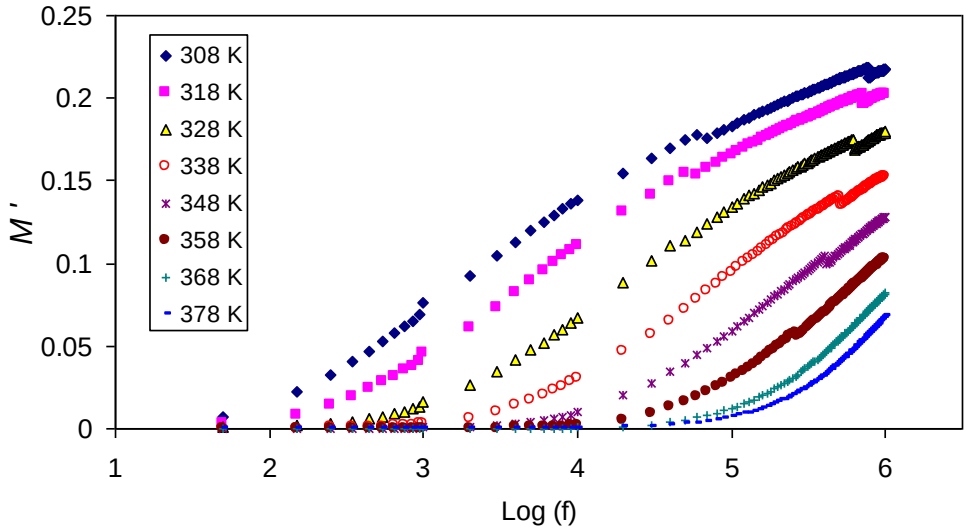

Figure 5. Frequency dependence real part (M′) of M* for CS:LiTf system at different temperature.

The frequency dependence of the imaginary part of the electric modulus at various temperatures for the sample displaying the highest dielectric constant (92:8) is illustrated in Figure 6.

The relaxation peak of the M″ spectra is apparent, indicating that ionic movements and polymer segmental movements are well-coupled manifesting peak in the M″ spectra [48], without a corresponding feature in ε″ spectra[49, 50], as shown in Figure 2. Such peaks are the transition regions from long range ionic mobility (translation) to short range mobility (dipolar); in other words, the carriers are restricted to potential wells being mobile across a limited distance at higher frequencies [51, 52]. Furthermore, the increase in temperature causes a decrease in conductivity relaxation time, as deduced from the shifting of the M″ spectra maximum peak frequencies in the forward direction with temperature. It is also worth noting that a key feature of the M″ spectra is that, if the migration of free ions in the polymer is the sole cause of conductivity while viscoelastic and dipolar relaxations have no impact, the related peak will be a Debye-like [53]. However, this study does not indicate the occurrence of such a feature, meaning that samples have non-Debye type behaviour. The Argand plots must be examined at various temperatures in order to improve that the relaxation dynamic is attributed to viscoelastic relaxation or due to ionic conductivity relaxation. Typically, the stretched exponential decay function of the electric field provides a characterisation of the broad and asymmetrical shape of electric modulus (M″) [54] as

$$\phi = \exp\left[\left(-\frac{t}{\tau}\right)^{\beta}\right] 0<\beta<1, \qquad (5)$$

In the above, β represents the stretching parameter and it is equal to 1.14/w, with w denoting the full-width at half-maximum (FWHM) and having a value of 1.14 in the case of Debye relaxation.

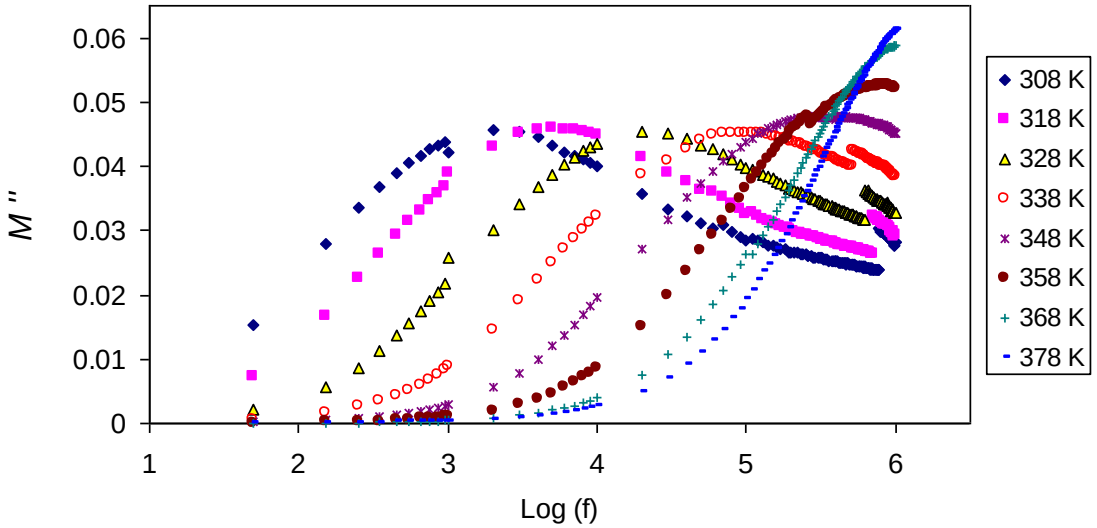

Figure 6. Frequency dependence imaginary part (M″) of M* for chitosan:lithiumtriflate (92:8) at different temperature.

The region where the maximum peak occurs is more quantitatively characterized as the condition in which $2\pi f_{max}=1/\tau_{\sigma}$, with τ_{σ} and f_{max} respectively denoting the conductivity relaxation time and a frequency corresponding to M''_{max}. Figure 7 illustrates the maximum peak frequency as a

function of temperature. The frequency-temperature relationship satisfies the Arrhenius behavior with the activation energy, E_a= 1.29 eV. Furthermore, every point lies on a nearly straight line, as suggested by the regression value R^2 of 0.98.

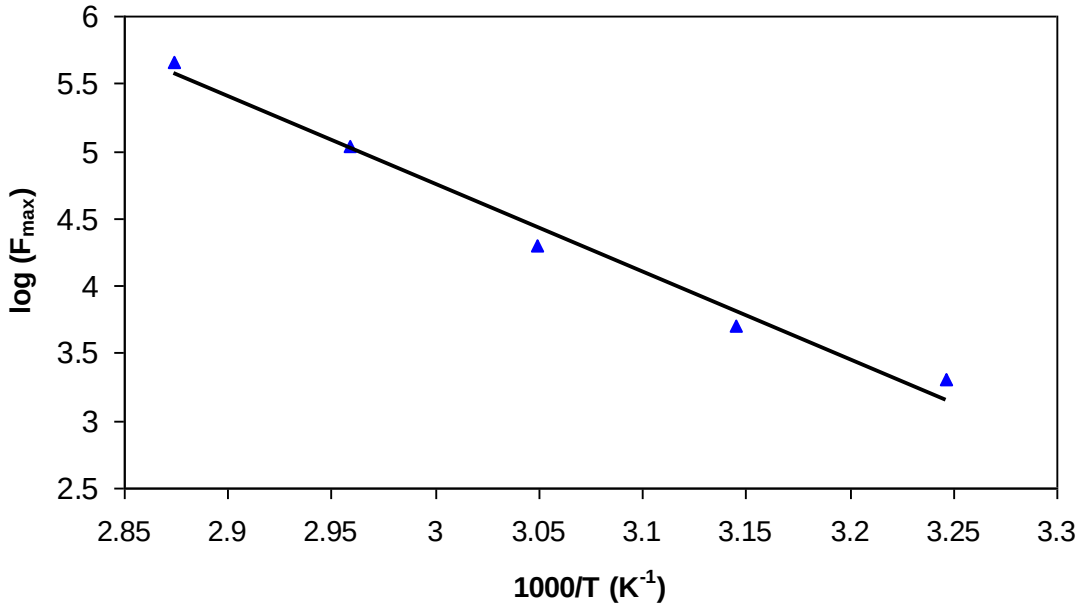

Figure 7. Arrhenius plots of the frequency at the maximum value of the imaginary part of electric modulus.

Normalizing of the electric modulus can provide more details about the reliance of the relaxation dynamics on the temperature, structure, as well as on the charge carriers' concentration [55]. The M''_{max} and f_{max} are used as a normalized variables for normalizing M'' and f respectively for the CS:LiTf system at various temperatures as shown in Figure 8.

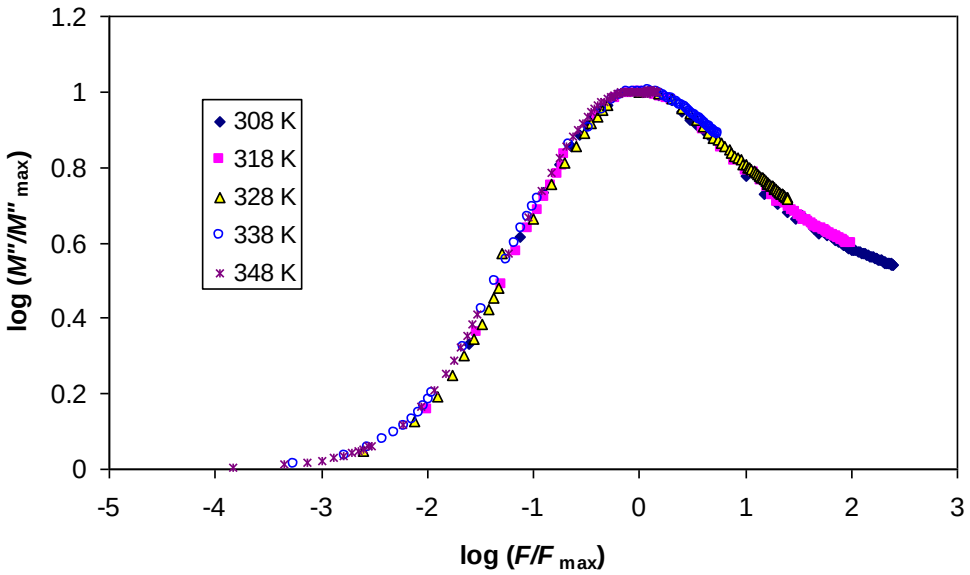

Figure 8. Plots of M''/M''_{max} vs log (f/f_{max}) for CS:LiTf at different temperature.

A master curve is created by the complete overlap of the curves for each temperature and it reflects the lack of temperature dependence of the dynamic relaxation processes for a given composition [56]. However, this finding contradicts the finding reported by Funke et al [57], who did not achieve a master curve for *M″* scaling spectra in the case of potassium thioborate ion conducting glasses. Meanwhile, in the present study, the master curve is helpful in understanding the dielectric processes taking place in the material. In the system employed, full width at half maximum (FWHM) has a greater value compared to the ideal Debye behavior (2.8 decades vs 1.14 decades). Furthermore, the conductivity relaxation is highly non-exponential, as suggested by the β value of 0.41 for the present system [58]. The smaller the value of β(0.41) larger is the relaxation deviation in respect of Debye-type relaxation (β = 1). It is obvious that, in the case of a practical solid electrolyte, β has a value smaller than 1 [59].

3.3.2 Relaxation process

There are two methods to demonstrate that the relaxation dynamic is belongs to viscoelastic relaxation or due to conductivity relaxation in chitosan-$LiCF_3SO_3$ based solid electrolyte.

.

Method 1: Argand analysis

In the polymer electrolyte used in this study, the nature of relaxation processes can be determined by examining Argand plots at various temperatures. The Argand curves at various temperatures are illustrated in Figure 9.

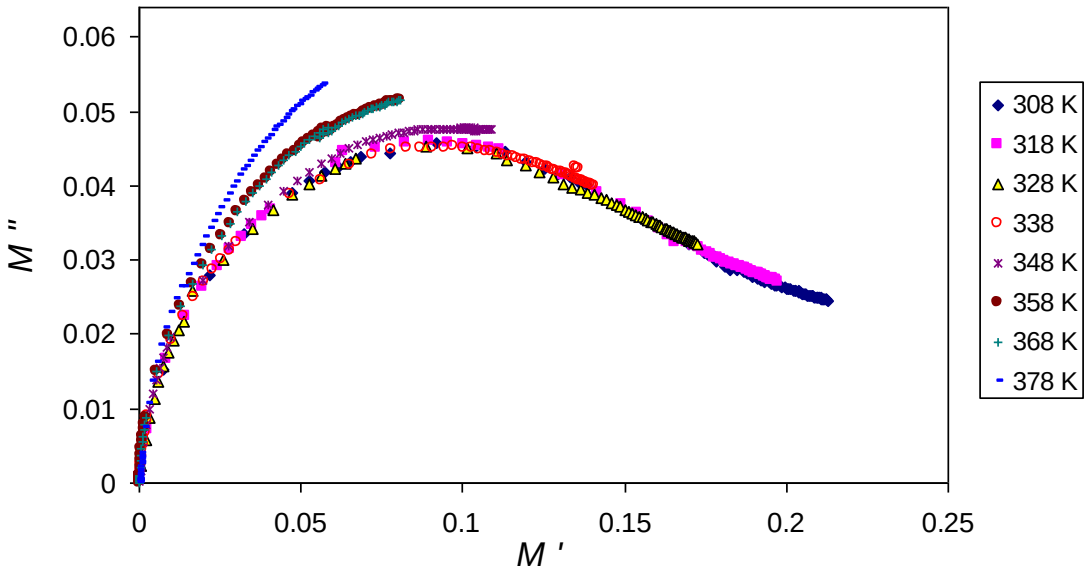

Figure 9. Argand plots for chitosan-lithium triflat at different temperatures.

Figure 9 clearly shows that the Argand plot curves take the form of incomplete half-semicircle resembling an arc, which cannot be clarified by the Debye model (i.e, single relaxation time). Thus, a distribution of relaxation time is required to elucidate the experimental data due to the fact that a larger number of dipoles and ions are activated and participated in the dielectric relaxation as temperature rises and thus a distribution of relaxation times. It is apparent that the Argand curves shift toward the origin as temperature rises. This can be ascribed to the increase of conductivity as result of increasing ionic mobility as temperature rises, which leads to Z' and Z" decrease. As interpreted by Mohomed et al [60], if the Argand plots (M″ vs M′) exhibit a complete semi-circular shape, the relaxation is due to the conductivity relaxation dynamic (pure ionic relaxation), while viscoelastic relaxation is the cause of relaxation under different circumstances. It is obvious that the present Argand plots display incomplete semi-circular behavior, meaning that the relaxation process is due to viscoelastic relaxation dynamic.

Method 2: log M" and log M' vs log f

The dependence of log M′ and log M″ on frequency in the conductivity relaxation region for chitosan-lithium triflate (92:8) at 328K are illustrated in Figures 10 and 11, respectively. As demonstrated in previous studies, the slopes of the log M′ and log M″ versus log f must be 1 and 2, respectively, for conductivity relaxation (pure ionic relaxation) [60, 61]. In contrast to the above assumptions, in the present work, the values obtained for the slopes of log M′ and log M″ versus log f are 0.78 and 0.44 respectively, i.e., the slope values are less than 1 for both cases.

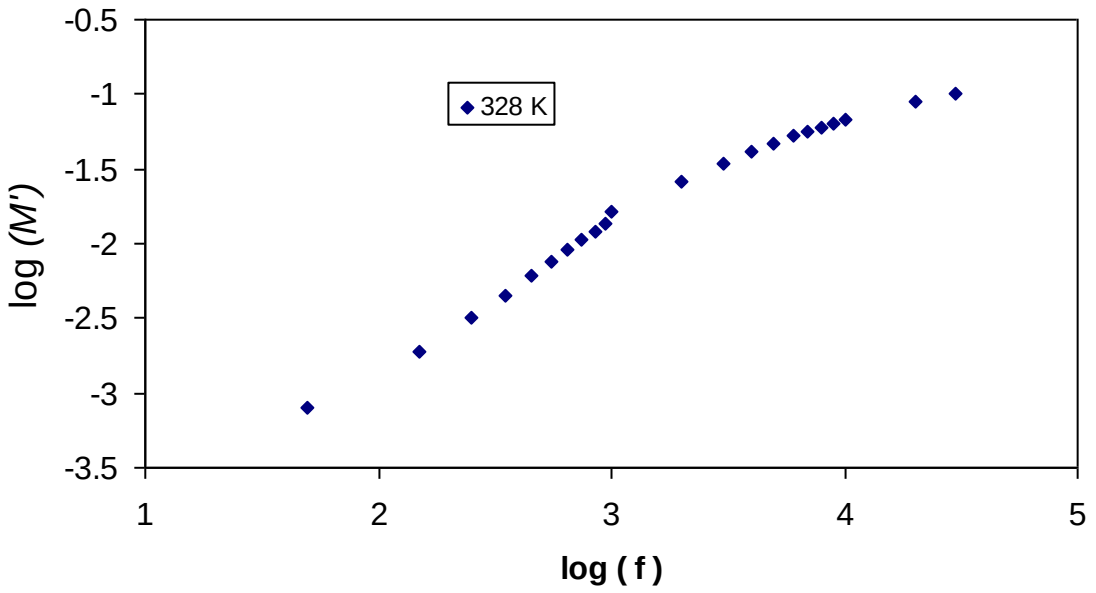

Figure 10. log *M'*vs log frequency for the chitosan-lithium triflat at the conductivity relaxation region

From the experimental analysis of method 1 and method 2, we conclude that, the relaxation process for chitosan-lithium triflate solid electrolyte is due to viscoelastic relaxation process rather

than conductivity relaxation. The interpretation of the findings rests on the fact that, in solid polymer electrolytes, ion transport is supported by large-scale segmental polymer chain motions, which not only break and renew coordination bonds required for cation transport, but also supply the free volume necessary for anion transport [62]. Thus, the relaxation dynamics can be ascribed to the strong coupling between the ionic and polymeric segmental motion.

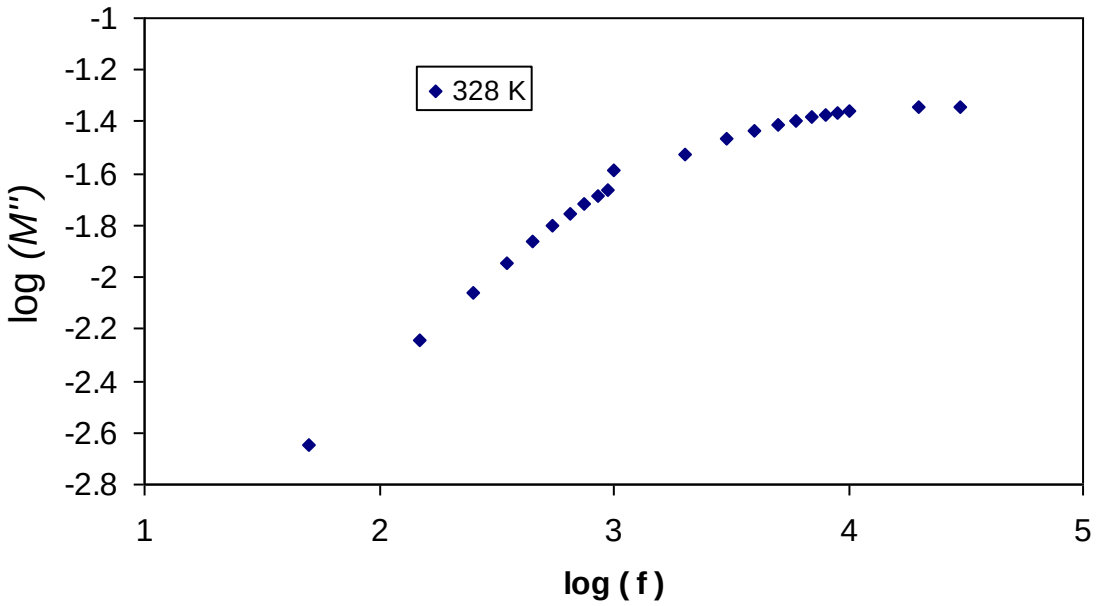

Figure 11. log *M″*vs log frequency for the chitosan-lithium triflat at the conductivity relaxation region.

4. CONCLUSION

The high values of dielectric constant (ε′) and dielectric loss (ε″) at low frequency can be ascribed to electrode polarization phenomena. The contribution of DC conductivity to dielectric loss (ε″) spectra is responsible for the absence of the relaxation peak. The decrease of both ε′ and ε″ at higher temperatures can be ascribed to the thermal degradation of chitosan-based solid electrolyte as a result of water desorption. The real part of electrical modulus shows that CS:LiTf systems are highly capacitive. The asymmetric peak of the imaginary part (*M″*) of electric modulus confirms the non-Debye type of relaxation for CS:LiTf systems. The master curve obtained from the scaling of *M″* spectra at various temperature was helpful in understanding the dielectric processes taking place in the CS:LiTf electrolyte. The scaling behaviour and the calculated value of β (0.57) indicate the non-exponential electrical relaxation. The temperature dependence of the conductivity relaxation time (τ_σ) follows the Arrhenius equation. The incomplete semicircle of Argand plot (*M″* vs *M′*) and the slope values of log *M″* and log *M′* vs log f (0.78, 0.44) suggests the viscoelastic relaxation dynamic of the CS:LiTf-based solid electrolyte.

ACKNOWLEDGEMENT
The authors gratefully acknowledge the financial support for this study from Ministry of Higher Education and Scientific Research-Kurdish National Research Council (KNRC), Kurdistan Regional Government/Iraq. The financial support from the University of Sulaimani and Komar Research Center (KRC), Komar University of Science and Technology are greatly appreciated.

References

1. S. B. Aziz, M.F.Z. Kadir and Z.H.Z. Abidin, *Int. J. Electrochem. Sci.*, 11(2016) 9228.
2. S. B. Aziz, W. O. Karim, K. W. Qadir and Q. Zafar, *Int. J. Electrochem. Sci.*, 13 (2018) 6112.
3. S. B. Aziz, O. Gh. Abdullah, S. R. Saeed and H. M. Ahmed, *Int. J. Electrochem. Sci.,* 13 (2018) 3812.
4. N.S. Salleh, S. B. Aziz, Z. Aspanut and M.F.Z. Kadir, *Ionics*, 22 (2016) 2157.
5. S. B Aziz, O. Gh. Abdullah and S. A. Hussein, *J. Electron. Mater.*, 47 (2018) 3800.
6. R. Hirase, Y. Higashiyama, M. Mori, Y. Takahar and Ch. Yamane, *Carbohydr. Polym.,* 80 (2010) 993
7. T. Si Trung, W. W. Thein-Han, N. T. Qui, Ch.-H. Ng and W. F. Stevens, *Bioresour. Technol.,* 97 (2006) 659.
8. P. Agrawal, G. J. Strijkers and K. Nicolay, *Adv. Drug Delivery Rev.*, 62 (2010) 42
9. S. B. Aziz and Z.H. Z. Abidin, *J. Soft Matter, Volume* 2013 (2013 0, Article ID 323868, 8 pages
10. M. Cheng, J. Deng, F. Yang, Y. Gong, N. Zhao and X. Zhang, *Biomater.*, 24 (2003) 2871.
11. N. M. El-Sawy, H. A. Abd El-Rehim, A. M. Elbarbary and El.-S. Hegazy, *Carbohydr. Polym.,* 79 (2010) 555.
12. H. Nagahama, H. Maeda, T. Kashiki, R. Jayakumar, T. Furuike and H. Tamura, *Carbohydr. Polym.,* 76 (2009) 255
13. S. B. Aziz, T. J. Woo, M. F.Z. Kadir and H. M. Ahmed, *J. Sci.: Adv. Mater. Devices*, 3 (2018) 1.
14. S. B. Aziz and Z.H. Z. Abidin, *J. Appl. Polym. Sci*., 132 (2015) 41774.
15. S. B. Aziz, *Appl. Phys.* A, 122 (2016) 706.
16. S. B. Aziz, *Iran Polym. J., 22 (*2013) 877.
17. K.P. Singh and P.N.Gupta, *Eur. Polym. J.*, 34 (1998) 1023.
18. S. B. Aziz, Z.H.Z. Abidin and A.K. Arof, *Physica B*, 405 (2010) 4429.
19. S. B. Aziz, Z.H.Z. Abidin and M.F.Z. Kadir, *Phys. Scr*., 90 (2015) 035808 (9pp)
20. M. E. Bassiouni, F. Al-Shamy, N. K. Madi and M. E. Kassem, *Mater. Let.*, 57 (2003) 1595.
21. M. Sugiura, A. Murase and T. Mitsuoka, *Polym. Degrad. Stab*. 27 (2001) 393.
22. M. Okutan and E. Şentürk, *J. Non-Cryst. Solids*, 357 (2008) 1526.
23. Kh. M. Batoo, Sh. Kumar., Ch. G. Lee and Alimuddin, *Curr. Appl Phys.*, 9 (2009) 1397.
24. A. S. A. Khiar, R. Puteh and A. K. *Arof, Physica* B, 373 (2006) 23-27
25. K. P Padmasree and D. K. Kanchan, *Mater. Sci. Eng., B*122 (2005) 24.
26. S. B. Aziz, O. Gh. Abdullah, S. A. Hussein and H. M. Ahmed, *Polymers*, 9 (2017) 622
27. S. B. Aziz, R. M. Abdullah, M. A. Rasheed and H. M. Ahmed, *Polymers*, 9 (2017) 338.
28. S. B. Aziz, M. A. Rasheed and Z. H. Z. Abidin, *J. Electron. Mater.*, 46 (2017) 6119.
29. R. Kunanuruksapong and A. Sirivat, *Appl. Phys. A,* 92 (2008) 313.
30. S. B. Aziz, *Bull. Mate.r Sci*., 38 (2015) 1597.
31. O. Gh. Abdullah, S. B. Aziz and M. A. Rasheed, *Ionics*, 24 (2018) 777.
32. S. B. Aziz and Z. H. Z. Abidin, *Mater. Chem. Phys.*, 144 (2014) 280.
33. S. M. Salem, *J. Mater. Sci*., 44 (2009) 5760.
34. B. H. Venkataraman and K. B. R. Varma, *Solid State Ionics*, 167 (2004) 197.
35. S. B. Aziz, O. Gh. Abdullah and M. A. Rasheed, *J, Mater, Sci,: Mater, Electron*., 28 (2017) 12873.
36. D. K. Das-Gupta, *J. Electrostatics*, 51-52 (2001) 159.

37. M. S. Kumar and D. K. Bhat, *Physica* B, (2009) 1143.
38. A. E. Bekheet and N. A. Hegab, *Vacuum*, 83 (2009) 391.
39. C. G. T. Netoa, J. A. Giacomettib, A. E. Jobb, F. C. Ferreirab, J. L. C. Fonsecaa and M. R. Pereira, *Carbohydr. Polym.,* 62 (2005) 97.
40. L. S. Ng and A. A. Mohamad, *J. Membr. Sci.,* 325 (2008) 653.
41. S. B. Aziz and S. M. Mamand, ,*Int. J. Electrochem. Sci*., 13 (2018)10274–10288
42. S. B. Aziz, *Adv. Mater. Sci. Eng., Volume* 2016 (2016), Article ID 2527013, 11 pages
43. S. B. Aziz, *J. Inorg. Organomet. Polym*., 28 (2018) 1942.
44. S.B. Aziz, Z.H.Z. Abidin and A.K. Arof, *eXPRESS Polym. Lett.*, 4 (2010) 300.
45. S. L. Agrawal, M. Singh, M. Tripathi, M. M. Dwiedi and K. Pandey, *J. Mat. Sci*., 44 (2009) 6060.
46. S. B. Aziz and R. M. Abdullah, *Electrochim. Acta*, 285 (2018) 30.
47. S. B. Aziz, S. Al-Zangana and O. Gh. Abdullah, *Int. J. Electrochem. Sci.,* 14 (2019)1909.
48. R. J. Sengwa, S. Choudhary and S. Sankhla, *eXPRESS Polym. Lett.,* 2 (2008) 800.
49. S. B. Aziz, S. Al-Zangana, H. J. Woo, M. F. Z. Kadir and O. Gh. Abdullah, *Results Phys.*, 11 (2018) 826.
50. M. H. Hamsan, M. F. Shukur, S. B. Aziz and M. F. Z. Kadir, *Bull. Mater. Sci.,* 42 (2019) 57.
51. J. Castillo, M. Chacon, R. Castillo, R. A. Vargas, P. R. Bueno and J. A. Varela, *Ionics*, 15 (2009) 537.
52. S. B. Aziz, R. M. Abdullah, M. F. Z. Kadir and H. M. Ahmed, *Electrochim. Acta*, 296 (2019) 494.
53. A. Bello, E. Laredo and M. Grimau, *J. Non-Cryst. Solids*, 353 (2007) 4283.
54. Ch. V. S. Reddy, X. Han, Q.-Y. Zhu, L.-Q. Mai and W. Chen, *Microelectron. Eng.*, 83(2006) 281.
55. A. Karmakar, S. Majumdar and S. Giri, *Phys. Rev. B: Condens. Matter*, 79 (2009) 094406.
56. C. R. Mariappan and G. Govindaraj, *Physica* B, 353 (2004) 65.
57. D. L. Sidebottom, B. Roling and K. Funke, *Phys. Rev. B: Condens. Matter*, 63 (2000) 024301.
58. S. Bhattacharya and A. Gosh, *Solid State Ionics*, 176 (2005) 1243.
59. M. Ram and S. Chakrabarti*, J. Alloys Compd.*, 462 (2008) 214.
60. K. Mohomed, T. G. Gerasimov, F. Moussy and J. P. Harmon, *Polymer*, 46 (2005) 3847.
61. H. W. Starkweather and P. Avakian, *J. Polym. Sci., Part B: Polym. Phys.*, 30 (1992) 637.
62. M. Marzantowicz, J.R. Dygas, F. Krok, Z. Florjańczyk and E. Zygadło-Monikowska, *J. Non-Cryst. Solids*, 353 (2007) 4467.